

Non-linear Power Spectrum including Massive Neutrinos: the Time-RG Flow Approach

Julien Lesgourgues,^{1,2,3} Sabino Matarrese,^{4,5} Massimo Pietroni,⁵ Antonio Riotto^{1,5}

¹*CERN, PH-TH Division, CH-1211, Geneve 23, Switzerland*

²*Ecole Polytechnique Fédérale de Lausanne, FSB/ITP/LPPC, BPS, Ch-10155, Lausanne, Switzerland*

³*LAPTH, Université de Savoie, CNRS, B.P. 110, F-74941, Annecy-le-Vieux Cedex, France*

⁴*Dipartimento di Fisica, Università di Padova, Via Marzolo, 8 - I-35131 Padua - Italy*

⁵*INFN, Sezione di Padova, Via Marzolo, 8 - I-35131 Padua - Italy*

(Dated: October 24, 2018)

Future large scale structure observations are expected to be sensitive to small neutrino masses, of the order of 0.05 eV or more. However, forecasts are based on the assumption that by the time at which these datasets will be available, the non-linear spectrum in presence of neutrino mass will be predicted with an accuracy at least equal to the neutrino mass effect itself, i.e. about 3%. Motivated by these considerations, we present the computation of the non-linear power spectrum of Λ CDM models in the presence of massive neutrinos using the Renormalization Group (RG) time-flow approach, which amounts to a resummation of perturbative corrections to the matter power spectrum to all orders. We compare our results with those obtained with other methods, i.e. linear theory, one-loop perturbation theory and N-body simulations and show that the time-RG method improves the one-loop method in fitting the N-body data, especially in determining the suppression of the matter power spectrum when neutrino are massive with respect to the linear power spectrum.

PACS numbers: 98.80.Cq

I. INTRODUCTION

The detection of atmospheric neutrino oscillations proves that at least one neutrino mass eigenstate is as heavy as approximately $(2.4 \pm 0.1 \times 10^{-3} \text{eV}^2)^{1/2}$. In the inverted hierarchy scenario, two eigenstates would have such a large mass, while in the degenerate scenario, the three masses would be of this order of magnitude or larger (for a recent analysis of the data, see e.g. [1]). In all cases, the total mass $M_\nu \equiv \sum m_\nu$ should be greater than approximately 0.05 eV. This means that neutrino masses are expected to impact significantly the cosmological evolution during matter and dark energy domination, first by enhancing the background neutrino density (today, $\Omega_\nu = (M_\nu/93.14 \text{eV})h^{-2} \gtrsim 10^{-3}$, instead of $\Omega_\nu = 1.712 \times 10^{-5}h^{-2}$ in the massless limit) [2], and more importantly, by reducing the growth rate of matter perturbations on comoving wavenumbers larger than $k_{\text{nr}} \simeq 2 \times 10^{-3}h/\text{Mpc}$. In the linear theory, this effect is maximal for $k \gtrsim 1h/\text{Mpc}$ and suppresses the current matter power spectrum (PS) by a factor $(1 - 8\Omega_\nu/\Omega_m)$, i.e. at least by 3% [3, 4].

At the moment, the most robust cosmological bounds on the total neutrino mass $M_\nu = \sum m_\nu$ rely either on its background effect (Komatsu et al. [5] obtain $M_\nu < 0.67 \text{eV}$ [95% C.L.] with WMAP-5, BAO and SNIa data only), or on limits on the suppression of the matter PS in the linear regime (Tegmark et al. [6] obtain $M_\nu < 0.9 \text{eV}$ [95% C.L.] using the combination of WMAP-3 with the PS of SDSS-LRG in the range $0.01 < k < 0.2h/\text{Mpc}$, after marginalization over an unknown nuisance parameter describing non-linear effects in the range $0.1 < k < 0.2h/\text{Mpc}$). In order to improve significantly these limits, it would be crucial to model the effect of neutrino masses in the non-linear regime, in order to include smaller scales in the analysis and increase the lever arm. For galaxy redshift surveys, including wavenumbers above $k \gtrsim 0.1h/\text{Mpc}$ remains a delicate issue, because in addition to non-linear corrections to the theoretical matter PS, one should be able to predict the scale-dependence of the light-to-mass bias, which starts to play a role on those scales. However, the prospects for neutrino mass determination are particularly encouraging thanks to other types of experiments. For instance, future weak lensing surveys (combined eventually with CMB lensing measurements) might reach a sensitivity of $M_\nu \sim 0.04 \text{eV}$ ($2\text{-}\sigma$) according to [7] (see also [8, 9, 10, 11]). These measurements – which are not affected by any light-to-mass bias – can probe the matter PS up to $z \sim 3$, which means, first, that they are likely to detect the non-trivial redshift dependence of the small-scale matter PS in the presence of massive neutrinos; and second, that they can measure cosmological fluctuations deeper in the linear regime than observations limited to small redshifts. Nevertheless, the forecasts of [7, 8, 9] do include non-linear scales, corresponding to multipoles $\ell < 1000$ in the case of [7] (for comparison, non-linear effects are important at $\ell > 40$ for sources with $z_s \sim 0.2$, and $\ell > 200$ for $z_s \sim 3$). Hence, they are based on the assumption that by the time at which these datasets will be available (of the order of one decade), the non-linear spectrum in the presence of neutrino mass will be predicted with an accuracy at least equal to the neutrino mass effect itself, i.e. about 3%. The same comment applies to other promising forecasts related to future cluster surveys [12], 21cm surveys [13, 14], high-redshift galaxy surveys [15], CMB-weak lensing cross-correlation [16, 17] or Lyman- α forest data [18]. In the latter case, one should model the effect of neutrino mass

not only on the total matter power spectrum, but also on the thermodynamical evolution of the intergalactic medium: hence, massive neutrinos should be implemented in hydrodynamical simulations of structure formation before deriving robust bounds on neutrino masses. All previous neutrino mass bounds from Lyman- α forest data neglected this issue.

Current weak lensing data probe the matter PS on much smaller scales than the previously discussed experiments (typically of the order of $k \sim (10 - 40) h/\text{Mpc}$). In this case, neutrino mass bounds have been obtained using the HALOFIT approach in order to compute non-linear corrections to the CDM component of the total power spectrum [19, 20]. The HALOFIT algorithm was derived and calibrated for the ΛCDM model. Its use in presence of massive neutrinos might be correct, but this would need further justification (see [21]).

Finally, the computation of the non-linear PS in presence of massive neutrinos would be important for CMB physics. A crucial issue in CMB observations is to deal with foreground contamination. In particular, the thermal SZ effect is difficult to remove, and a large fraction of it will contribute to the final measured temperature spectrum. This SZ effect depends on the non-linear PS; hence, it can be computed and fitted at the same time as primary anisotropies. However, any mistake in the computation of this contribution would result in a significant bias on the cosmological parameters (for instance, on the scalar spectral tilt) [22]. Even with the smallest allowed neutrino mass, the SZ spectrum should be sensitive to neutrino free-streaming on small scales. So, if the CMB spectrum of a precise experiment like Planck was analysed using SZ spectrum computations in which neutrino mass effects are neglected, the bias induced on cosmological parameters might be significant. Note that instead of fitting this component, one can marginalize over nuisance parameters accounting for its amplitude and slope, or just restrict the multipole range used in the analysis, but this is at the expense of reducing the parameter sensitivity [22]. Hence, investigating the effect of neutrino masses on non-linear cosmological perturbations is also important in order to push the precision of CMB observations on all cosmological parameters.

For all these reasons, a crucial step for precision cosmology is to incorporate free-streaming massive neutrinos in numerical or analytical estimates of the non-linear matter PS on small scales. On the side of numerical simulations, the first steps were performed in [23, 24, 25, 26]. To our knowledge, other attempts to simulate mixed cold plus hot models were treating neutrinos as extra cold particles with a different initial PS. This approach neglects the effect of neutrino thermal velocities, and fails to reproduce even the linear evolution. Ref. [25] shows explicitly that neglecting thermal velocities results in an error which is of the same size as the very effect of a small neutrino mass: this makes current bounds on m_ν from Lyman- α data suspicious. However, implementing free-streaming neutrino “particles” in simulation is very demanding, because of the large number of particles required to sample the full neutrino phase space, and of the tiny time steps needed to follow the particle trajectories with sufficient accuracy, because of their large velocities. Some significant progress can be expected in this field in the next years.

In parallel, it is important to derive analytic approximations of the non-linear evolution in order to cross-check the results from simulations, to reach eventually smaller scales and larger redshifts, and hopefully to obtain computationally faster ways of predicting non-linear spectra. Various analytical schemes have been discussed in the past years for ΛCDM models, inspired by quantum field theory; these include one-loop calculations [27, 28, 29], resummation techniques [30, 31, 32], renormalization group approaches [33, 34, 35, 36, 37, 38, 39], or the Time Renormalization Group (TRG) flow calculation of [40].

The first attempt to incorporate massive neutrinos in these calculations was performed by Saito et al. [41], who provide a first-order approximation of the one-loop computation. The full one-loop results were obtained by Wong [42]. The goal of this paper is to generalize the method of [40] in the presence of neutrino masses, and to compare with previous results from [25, 41, 42]. In this new approach the matter power spectrum, the bispectrum (*i.e.* the connected three point-correlation function in Fourier space) and higher order correlations, are obtained – at any redshift and for any momentum scale – by integrating a system of differential equations. Truncating at the level of the trispectrum (*i.e.* the connected four point-correlation function in Fourier space), the solution of the equations corresponds to the summation of an infinite class of perturbative corrections. In the diagrammatic language, this is equivalent to resumming at all orders in perturbation theory the corrections to the matter power spectrum. Furthermore, comparison with N-body simulations for zero neutrino masses shows that the method is valid up to momentum wavenumbers of the order of $0.3 h/\text{Mpc}$ at $z = 1$, and able to describe the non-linearities due to mode-to-mode coupling in the baryon acoustic oscillations region. Compared to other resummation frameworks, this scheme is particularly suited to cosmologies other than ΛCDM , such as those based on modifications of gravity and those containing massive neutrinos.

The paper is organized as follows: in Section 1 we summarize our method based on Ref. [40] generalized to include massive neutrinos. In Section 3 we present our numerical findings and compare them with those obtained with other methods, namely linear theory, one-loop perturbation theory [41, 42] and the N-body simulations of Refs. [26].

II. METHOD

Our goal is to set up a method to compute non-linear corrections to the matter PS in a mixed dark matter (MDM) model. The matter density fluctuation is given by

$$\delta_m \equiv (\delta\rho_c + \delta\rho_b + \delta\rho_\nu)/\bar{\rho}_m = (1 - f_\nu)\delta_{cb} + f_\nu\delta_\nu, \quad (1)$$

where the subscripts ‘c’, ‘b’, ‘ ν ’, and ‘cb’, stand for cold dark matter (CDM), baryons, neutrinos, and CDM plus baryons, respectively, and $f_\nu = \Omega_\nu/\Omega_m$. The total matter PS is then given by

$$P_m(k; z) = (1 - f_\nu)^2 P_{cb}(k; z) + 2(1 - f_\nu)f_\nu P_{cb,\nu}(k; z) + f_\nu^2 P_\nu(k; z). \quad (2)$$

In ref. [41] the expression above was approximated by using the linear order result for the $cb - \nu$ and the $\nu - \nu$ PS’s (the second and third terms in Eq. (2), respectively), while including non-linear corrections to the $cb - cb$ one in the so-called one-loop approximation, which includes density and velocity perturbations up to the third order [27]. In the present paper we will go beyond the one-loop approximation for P_{cb} , using the TRG approach of Ref. [40], while keeping the linear order results for the other two contributions to Eq. (2).

The TRG is a method to sum perturbative corrections to all orders. The starting point are the continuity and Euler equations satisfied by the density contrast and peculiar velocity of a non-relativistic fluid (*i.e.* CDM or baryons in the present case),

$$\begin{aligned} \frac{\partial \delta_{cb}}{\partial \tau} + \nabla \cdot [(1 + \delta_{cb})\mathbf{v}] &= 0, \\ \frac{\partial \mathbf{v}}{\partial \tau} + \mathcal{H}\mathbf{v} + (\mathbf{v} \cdot \nabla)\mathbf{v} &= -\nabla\phi, \end{aligned} \quad (3)$$

where τ is the conformal time and we have assumed $\delta_b = \delta_c = \delta_{cb}$. The gravitational potential ϕ is determined by the total mass fluctuation, via the Poisson equation

$$\nabla^2 \phi = \frac{3}{2} \mathcal{H}^2 \Omega_m \delta_m, \quad (4)$$

where $\mathcal{H} = d \log a / d\tau$. Dropping the $\delta_{cb}\mathbf{v}$ term in the continuity equation and the $(\mathbf{v} \cdot \nabla)\mathbf{v}$ one in the Euler equation, the solutions to the system above reproduce linear perturbation theory on the subhorizon scales we are interested in.

In order to close the system (3), we go to Fourier space, use Eq. (1), and approximate the RHS of the Poisson equation as follows

$$\frac{3}{2} \mathcal{H}^2 \Omega_m(\tau) \delta_m(\mathbf{k}, \tau) \simeq \frac{3}{2} \mathcal{H}^2 \Omega_{cb}^{eff}(\mathbf{k}, \tau) \delta_{cb}(\mathbf{k}, \tau), \quad (5)$$

where

$$\Omega_{cb}^{eff}(\mathbf{k}, \tau) \equiv \Omega_m(\tau)(1 - f_\nu) \left(1 + \frac{f_\nu \delta_\nu^L(\mathbf{k}, \tau)}{(1 - f_\nu) \delta_{cb}^L(\mathbf{k}, \tau)} \right). \quad (6)$$

$\delta_{\nu,cb}^L$ indicate the density perturbations evolved according to linear theory. Notice that, due to the different space dependence of δ_ν^L and δ_{cb}^L in the massive neutrino case, Ω_{cb}^{eff} – unlike Ω_m – is space-dependent. Another approximation is to recursively use the full TRG-evolved δ_{cb} fluctuation in Eq. (6). However, we numerically checked that performing one iteration (*i.e.*, using the output non-linear δ_{cb} as an input in Eq. (6) instead of δ_{cb}^L) does not affect the results by more than 0.1%. This way of including massive neutrinos is conceptually similar to the grid method used in N-body simulations of Ref. [26]. where, instead of simulating massive neutrinos as particles with individual velocities, they are embedded as a local neutrino density on a grid which is evolved in time using linear theory.

Next, we write Eqs. (3, 4) in a compact form [30, 40]. First, we introduce the doublet φ_a ($a = 1, 2$), given by

$$\begin{pmatrix} \varphi_1(\mathbf{k}, \eta) \\ \varphi_2(\mathbf{k}, \eta) \end{pmatrix} \equiv e^{-\eta} \begin{pmatrix} \delta_{cb}(\mathbf{k}, \eta) \\ -\theta(\mathbf{k}, \eta)/\mathcal{H} \end{pmatrix}, \quad (7)$$

where $\theta = i \mathbf{k} \cdot \mathbf{v}$, and the time variable has been replaced by the logarithm of the scale factor,

$$\eta = \log \frac{a}{a_{in}}, \quad (8)$$

a_{in} being the scale factor at a conveniently remote epoch, such that all the relevant scales are well inside the linear regime.

Then, we get

$$\partial_\eta \varphi_a(\mathbf{k}, \eta) = -\Theta_{ab}(\mathbf{k}, \eta)\varphi_b(\mathbf{k}, \eta) + e^\eta \gamma_{abc}(\mathbf{k}, -\mathbf{p}, -\mathbf{q})\varphi_b(\mathbf{p}, \eta)\varphi_c(\mathbf{q}, \eta), \quad (9)$$

where

$$\Theta(\mathbf{k}, \eta) = \begin{pmatrix} 1 & -1 \\ -\frac{3}{2}\Omega_{cb}^{eff}(\mathbf{k}, \eta) & 2 + \frac{d \log \mathcal{H}}{d\eta} \end{pmatrix}, \quad (10)$$

and the only non-vanishing elements of the *vertex* function $\gamma_{abc}(\mathbf{k}, \mathbf{p}, \mathbf{q})$ are

$$\begin{aligned} \gamma_{112}(\mathbf{k}, \mathbf{p}, \mathbf{q}) &= \frac{1}{2} \delta_D(\mathbf{k} + \mathbf{p} + \mathbf{q}) \frac{(\mathbf{p} + \mathbf{q}) \cdot \mathbf{q}}{q^2}, \\ \gamma_{222}(\mathbf{k}, \mathbf{p}, \mathbf{q}) &= \delta_D(\mathbf{k} + \mathbf{p} + \mathbf{q}) \frac{(\mathbf{p} + \mathbf{q})^2 \mathbf{p} \cdot \mathbf{q}}{2p^2q^2}, \end{aligned} \quad (11)$$

and $\gamma_{121}(\mathbf{k}, \mathbf{p}, \mathbf{q}) = \gamma_{112}(\mathbf{k}, \mathbf{q}, \mathbf{p})$.

In Eq. (9), repeated indices are summed over, and integration over momenta \mathbf{q} and \mathbf{p} is understood. Notice that all the information on the neutrino mass, both at the background and at the linear perturbation level, is contained in Θ_{21} , the other entries of Θ and the vertices being universal.

At this point we should stress a crucial difference between the present approach and the ones of refs. [30, 31, 34, 35]. Namely, in those papers, the equations are derived in the Einstein-deSitter (EdS) case ($\Omega_m = 1$) and then extended to different cosmologies, such as Λ CDM, by reinterpreting η as the logarithm of the linear growth factor, while keeping the equations unchanged. In particular, the Θ - matrix is approximated by that of the EdS model. It was discussed in [30] and numerically checked in [40] that in cosmologies with a constant equation of state for the dark energy, this procedure gives at most a $O(1\%)$ error at $z = 0$ for $k \gtrsim 0.3h/\text{Mpc}$, rapidly decreasing at higher redshift and larger scales. The physical reason for this accuracy lies in the fact that this procedure takes fully into account the growing mode of the non-EdS cosmology, while it mistreats the decreasing one. The latter start to play a role only at high k 's or for low redshifts, where non-linearities become important.

However, when massive neutrinos contribute to the dark matter, the linear growth factor is k -dependent, and the redefinition of η is ill-defined. This singles out the present approach, the TRG, as particularly suited to this case. Indeed, in this approach, we keep the same definition, Eq. (8) for any cosmological model, and take fully into account the k -dependence of the linear growth function via the $\Omega_{cb}^{eff}(\mathbf{k}, \eta)$ term in Eq. (10).

The evolution in η of the correlation functions of the φ_a fields can be derived by iterating the application of Eq. (9). The result is an infinite tower of coupled integro-differential equations. Following Ref. [40], we will truncate the system by neglecting the trispectrum. The evolution equations for the PS, $\langle \varphi_a(\mathbf{k}, \eta)\varphi_b(\mathbf{q}, \eta) \rangle \equiv \delta_D(\mathbf{k} + \mathbf{q})P_{ab}(\mathbf{k}, \eta)$, and for the bispectrum, $\langle \varphi_a(\mathbf{k}, \eta)\varphi_b(\mathbf{q}, \eta)\varphi_c(\mathbf{p}, \eta) \rangle \equiv \delta_D(\mathbf{k} + \mathbf{q} + \mathbf{p})B_{abc}(\mathbf{k}, \mathbf{q}, \mathbf{p}; \eta)$ are then given by

$$\begin{aligned} \partial_\eta P_{ab}(\mathbf{k}, \eta) &= -\Theta_{ac}(\mathbf{k}, \eta)P_{cb}(\mathbf{k}, \eta) - \Theta_{bc}(\mathbf{k}, \eta)P_{ac}(\mathbf{k}, \eta) \\ &\quad + e^\eta \int d^3q [\gamma_{acd}(\mathbf{k}, -\mathbf{q}, \mathbf{q} - \mathbf{k}) B_{bcd}(\mathbf{k}, -\mathbf{q}, \mathbf{q} - \mathbf{k}; \eta) \\ &\quad + B_{acd}(\mathbf{k}, -\mathbf{q}, \mathbf{q} - \mathbf{k}; \eta) \gamma_{bcd}(\mathbf{k}, -\mathbf{q}, \mathbf{q} - \mathbf{k})], \\ \partial_\eta B_{abc}(\mathbf{k}, -\mathbf{q}, \mathbf{q} - \mathbf{k}; \eta) &= -\Theta_{ad}(\mathbf{k}, \eta)B_{dbc}(\mathbf{k}, -\mathbf{q}, \mathbf{q} - \mathbf{k}; \eta) - \Theta_{bd}(-\mathbf{q}, \eta)B_{adc}(\mathbf{k}, -\mathbf{q}, \mathbf{q} - \mathbf{k}; \eta) \\ &\quad - \Theta_{cd}(\mathbf{q} - \mathbf{k}, \eta)B_{abd}(\mathbf{k}, -\mathbf{q}, \mathbf{q} - \mathbf{k}; \eta) \\ &\quad + 2e^\eta [\gamma_{ade}(\mathbf{k}, -\mathbf{q}, \mathbf{q} - \mathbf{k})P_{db}(\mathbf{q}, \eta)P_{ec}(\mathbf{k} - \mathbf{q}, \eta) \\ &\quad + \gamma_{bde}(-\mathbf{q}, \mathbf{q} - \mathbf{k}, \mathbf{k})P_{dc}(\mathbf{k} - \mathbf{q}, \eta)P_{ea}(\mathbf{k}, \eta) \\ &\quad + \gamma_{cde}(\mathbf{q} - \mathbf{k}, \mathbf{k}, -\mathbf{q})P_{da}(\mathbf{k}, \eta)P_{eb}(\mathbf{q}, \eta)]. \end{aligned} \quad (12)$$

The system is solved by giving initial conditions for the PS and the bispectrum at $\eta = 0$, and integrating forward in η . In the $a_{in} \rightarrow 0$ limit, the initial conditions can be obtained from linear perturbation theory,

$$\begin{aligned} P_{11}(\mathbf{k}, 0) &= P_{11}^L(\mathbf{k}, 0), \\ P_{12}(\mathbf{k}, 0) &= f_L(\mathbf{k}, 0)P_{11}^L(\mathbf{k}, 0), \\ P_{22}(\mathbf{k}, 0) &= f_L^2(\mathbf{k}, 0)P_{11}^L(\mathbf{k}, 0), \\ B_{abc}(\mathbf{k}, -\mathbf{q}, \mathbf{q} - \mathbf{k}; 0) &= 0, \end{aligned} \quad (13)$$

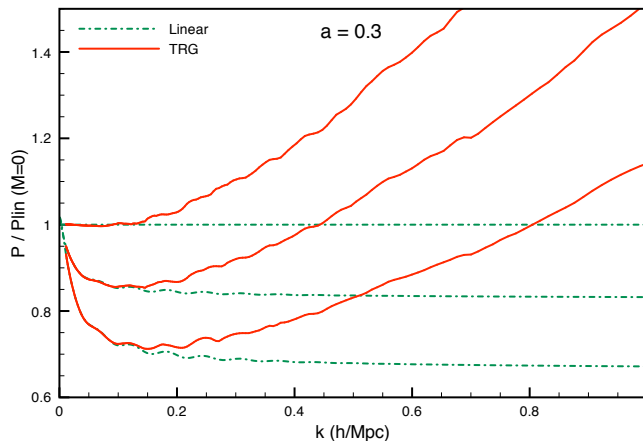


FIG. 1: Matter power spectra at $a = 0.3$ ($z = 2.33$) normalized to the linear one for $M_\nu = 0$. The red, solid lines are the result of the TRG method described in the text, while the green, dash-dotted ones are the linear approximation. The curves from top to bottom correspond to $M_\nu = 0, 0.3$, and 0.6 eV, respectively.

where the multiplication of the initial P_{12} and P_{22} by appropriate powers of the linear growth function, $f_L(\mathbf{k}, \eta) \equiv d \log \delta_{cb}^L(\mathbf{k}, \eta) / d \eta$, selects the linear growing mode. In our computations, we will use $a_{in} = 1/41$, and take the density-density power spectrum P_{11}^L from the Boltzman code CAMB [43]. More precisely, we extract P_{cb} , $P_{cb,\nu}$, P_ν and Ω_{cb}^{eff} at any value of (k, z) from the quantities δ_{cb} and δ_ν evolved by CAMB in the synchronous gauge.

Different approximations of the system above give the linear and the one-loop approximations, respectively. Indeed, the linear result for the PS is obtained simply by setting $B_{abc} = 0$, and integrating the first of Eqs. (12). On the other hand, the one-loop result is obtained by inserting the linear PS in the RHS of the second of Eqs. (12) and using the resulting B_{abc} in the first one.

Integrating the system above as it is, goes beyond the one-loop approximation, and corresponds to summing infinite perturbative contributions. As discussed in detail in Ref. [40], at each step in η the PS and the bispectrum appearing at the RHS's include non-linear corrections matured from $\eta = 0$ to η .

In the next section we will present the results of such integrations and compare them with the linear, the one-loop approximations and the N-body results.

III. RESULTS AND DISCUSSION

The impact of non-linear corrections on the linear PS is opposite with respect to that of a massive neutrino component. Indeed, while the latter damps the PS at scales larger than $k_{nr} \simeq 2 \times 10^{-3} h/\text{Mpc}$, non-linearities enhance it for $k \gtrsim k_{NL}$, where $k_{NL} \simeq 0.05 h/\text{Mpc}$ at $z = 0$ and scales roughly as $(1+z)^{2/3}$. The combination of both effects is shown in Fig. 1, where we plot the total matter PS normalized to the linear one for $M_\nu = 0$, at $a = 0.3$, *i.e.* $z = 2.33$ (a is the cosmological scale factor, normalized to $a = 1$ today). We have assumed a flat cosmological model with Hubble parameter $h = 0.70$, and density parameters $\Omega_\Lambda = 0.7$ and $\Omega_m = 0.3$. Ω_m is given by the sum of $\Omega_b = 0.05$ and $\Omega_c + \Omega_\nu$. The primordial power spectrum was assumed of the scale-invariant Harrison-Zel'dovich form ($n = 1$), normalized as to give $\sigma_8 = 0.878$ for $\Omega_\nu = 0$.

The green, dash-dotted lines are the linear approximation result, while the red ones were obtained with the TRG method. The curves from top to bottom correspond to $M_\nu = 0, 0.3$, and 0.6 eV, respectively. As we see, even at an intermediate redshift the effect of non-linearities overcomes that of massive neutrinos, turning a k -independent suppression in a k -dependent enhancement, which should be understood in order to derive reliable bounds on neutrino masses.

In the following figures we disentangle the non-linear from the massive neutrinos effects. Non-linear effects are shown in Fig. 2, where the total matter power spectra is divided by the linear one computed for the same value of the total neutrino mass. We compare results for $M_\nu = 0, 0.3$ and 0.6 eV obtained in one-loop perturbation theory (black dotted), and by the TRG method (red solid). Blue diamonds are the results of N-body simulations of Ref. [26], when neutrinos are treated like particles. The results are given for $a = 0.3$ corresponding to redshift $z = 2.33$ and $a = 0.5$ corresponding to $z = 1$.

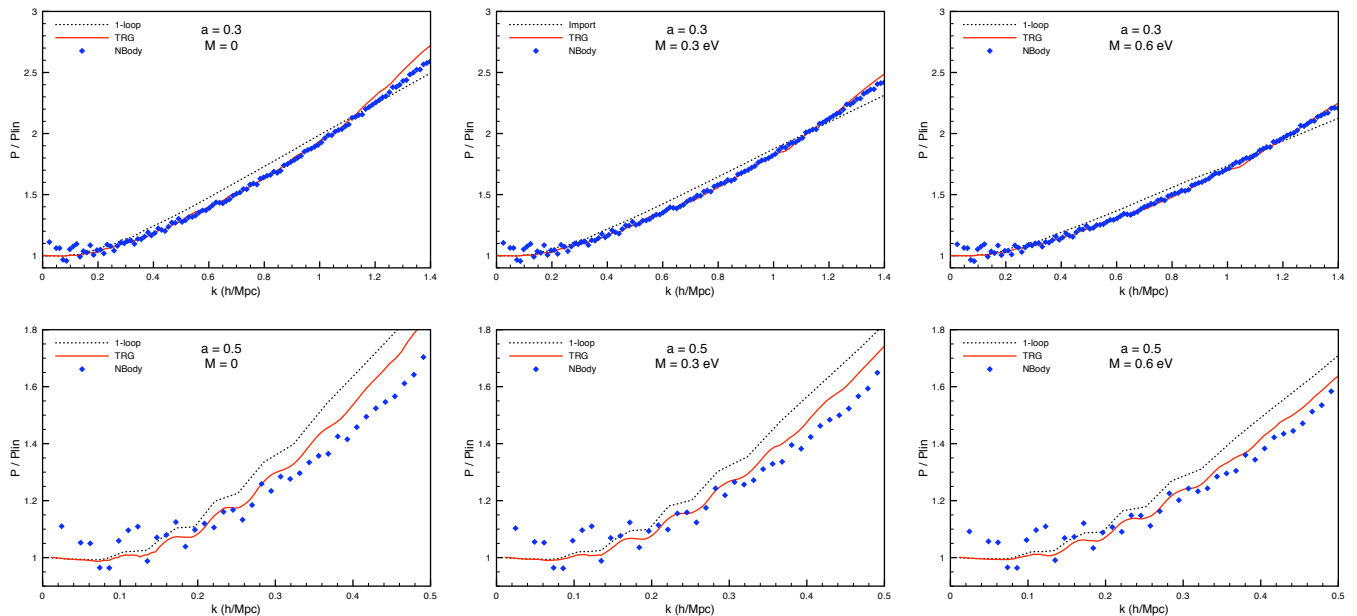


FIG. 2: Power spectra divided by the linear one for the same value of M_ν as computed in one-loop perturbation theory (black, dotted), and by the TRG method (red, solid). Blue diamonds are the results of N-body simulation of Ref. [26], when neutrinos are treated like particles.

At high redshift, the TRG method works surprisingly well in the whole range of k displayed in the figure, and is able to reproduce the N-body simulations better than the one-loop result, especially for large neutrino masses. For smaller redshifts, this tendency remains, but as expected, the agreement between the N-body simulation and the TRG method is valid only up to $k = 0.3h/\text{Mpc}$, while in the same range the one-loop method overestimates the non-linear to linear power spectra ratio. At both redshifts, the agreement with N-body simulations increases with the neutrino mass. This can be understood by recalling that we keep $\Omega_c + \Omega_\nu$ fixed, and non-linear effects decrease when the CDM component is lowered.

In Fig. 3 we show the effect of the neutrino mass as computed in linear approximation (green, dash-dotted line), one-loop perturbation theory (black, dotted), and by the TRG method (red, solid). Blue diamonds are again the results of N-body simulation of Ref. [26]. The upper (lower) group of lines corresponds to $M_\nu = 0.3$ (0.6) eV, respectively. From this figure, we can infer two things. On one hand, the relative change between massive and massless neutrino models is approximately the same for the TRG and the one-loop method. This is not surprising, because the difficulty of the one-loop method to reproduce the N-body data disappears in the plotted ratios. On the other hand, we see that both the one-loop and TRG method tend to over-estimate the impact of neutrino masses for small redshift. It should also be noticed that the simulations of Ref. [26], where the neutrinos are modeled by the grid approach, seem to be in closer agreement with us than those in which neutrinos are represented as particles (the blue diamonds in our plots), as could be expected from the conceptual similarity.

In this paper we have presented the derivation of the large scale matter power spectrum in the presence of massive neutrinos using the TRG method which resums the perturbative corrections to the matter power spectrum to all orders and therefore extends the one-loop computation. Evaluating numerically the TRG matter power spectrum, we have seen that nonlinear corrections enhance the suppression of the power spectrum at small scales due to the neutrino free-streaming. This enhanced suppression has been observed in N-body simulations [25, 26] and already appears at one-loop [42], but the TRG is in better agreement with N-body data, as it is manifested from Fig. 2.

Our results indicate that the TRG approach is particularly suited to describe intermediate scales, where linear theory and one-loop perturbation theory are not reliable, and, on the other hand, N-body simulations require very large volumes and are therefore extremely time consuming. This range of scales will be accurately measured by future galaxy surveys with the aim of pinning down the dark energy equation of state by measuring baryonic acoustic oscillations (BAO), from $k \simeq 0.05 h/\text{Mpc}$ to $0.3 h/\text{Mpc}$. In this context, it has been shown [31, 44] that non-linearities affect non-trivially the BAO feature by shifting the position of the peaks towards smaller scales with respect to those computed in linear theory. The same effect is witnessed by the wiggles in Figs. 2, which would not be there if the non-linear corrections were k -independent in that range of scales. Neutrino masses, modifying the non-linear corrections, also have an impact on the BAOs, and this is seen in our Figs. 3.

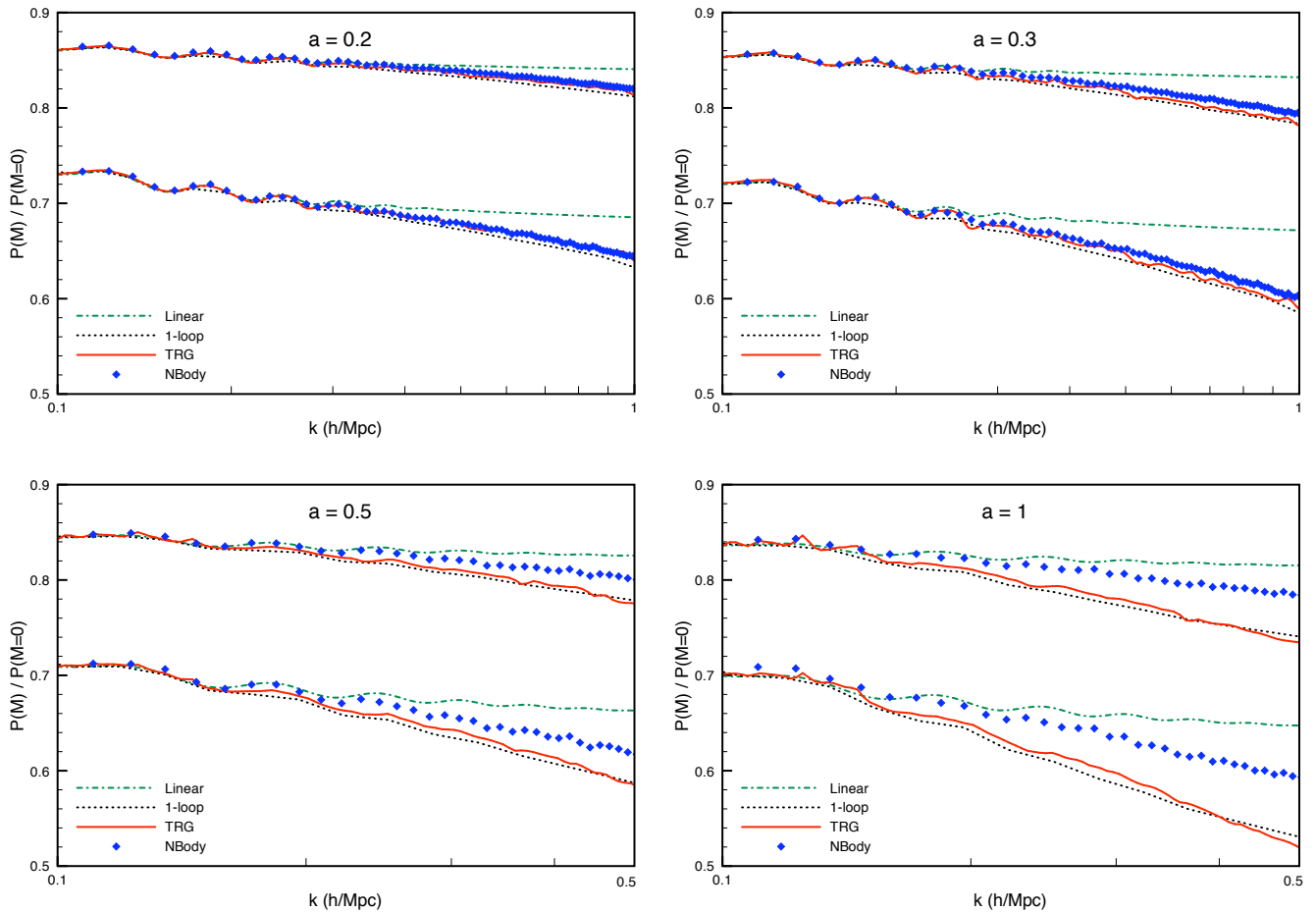


FIG. 3: Suppression on the total PS induced by non-zero neutrino masses at different epochs, as computed in linear approximation (green, dash-dotted line), one-loop perturbation theory (black, dotted), and by the TRG method (red, solid). Blue diamonds are the results of N-body simulation of Ref. [26]. The upper (lower) group of lines corresponds to $M_\nu = 0.3$ (0.6) eV, respectively.

The approach can be improved along two possible lines. On one side neutrino perturbations have been treated at the linear level; a nonlinear generalization would be of course welcome. On the other side, the TRG technique might be improved by including vertex corrections or, in other words, solving the equations for the correlators including the connected four-point correlation function.

Acknowledgments

We kindly thank S. Hannestad and J. Brandbyge for sending us the data relative to their N-body simulations with massive neutrinos of Ref. [26], and for comments on the manuscript. Precious comments from Y. Wong are also acknowledged. This research has been partially supported by ASI contract I/016/07/0 "COFIS" and by the European Community's Research Training Networks under contracts MRTN-CT-2004-50369 and MRTN-CT-2006-035505.

-
- [1] T. Schwetz, M. Tortola, and J. W. F. Valle (2008), 0808.2016.
 - [2] G. Mangano et al., Nucl. Phys. **B729**, 221 (2005), hep-ph/0506164.
 - [3] W. Hu, D. J. Eisenstein, and M. Tegmark, Phys. Rev. Lett. **80**, 5255 (1998), astro-ph/9712057.
 - [4] J. Lesgourgues and S. Pastor, Phys. Rept. **429**, 307 (2006), astro-ph/0603494.
 - [5] E. Komatsu et al. (WMAP) (2008), 0803.0547.

- [6] M. Tegmark et al. (SDSS), *Phys. Rev.* **D74**, 123507 (2006), astro-ph/0608632.
- [7] Y.-S. Song and L. Knox (2003), astro-ph/0312175.
- [8] S. Hannestad, H. Tu, and Y. Y. Y. Wong, *JCAP* **0606**, 025 (2006), astro-ph/0603019.
- [9] T. D. Kitching, A. F. Heavens, L. Verde, P. Serra, and A. Melchiorri, *Phys. Rev.* **D77**, 103008 (2008), 0801.4565.
- [10] J. Lesgourgues, L. Perotto, S. Pastor, and M. Piat, *Phys. Rev.* **D73**, 045021 (2006), astro-ph/0511735.
- [11] L. Perotto, J. Lesgourgues, S. Hannestad, H. Tu, and Y. Y. Y. Wong, *JCAP* **0610**, 013 (2006), astro-ph/0606227.
- [12] S. Wang, Z. Haiman, W. Hu, J. Khoury, and M. May, *Phys. Rev. Lett.* **95**, 011302 (2005), astro-ph/0505390.
- [13] S. Wyithe and A. Loeb (2008), 0808.2323.
- [14] J. R. Pritchard and E. Pierpaoli (2008), 0805.1920.
- [15] S. Hannestad and Y. Y. Y. Wong, *JCAP* **0707**, 004 (2007), astro-ph/0703031.
- [16] K. Ichikawa and T. Takahashi, *JCAP* **0802**, 017 (2008), astro-ph/0510849.
- [17] J. Lesgourgues, W. Valkenburg, and E. Gaztanaga, *Phys. Rev.* **D77**, 063505 (2008), 0710.5525.
- [18] S. Gratton, A. Lewis, and G. Efstathiou, *Phys. Rev.* **D77**, 083507 (2008), 0705.3100.
- [19] I. Tereno et al. (2008), 0810.0555.
- [20] K. Ichiki, M. Takada, and T. Takahashi (2008), 0810.4921.
- [21] K. Abazajian, E. R. Switzer, S. Dodelson, K. Heitmann, and S. Habib, *Phys. Rev.* **D71**, 043507 (2005), astro-ph/0411552.
- [22] O. Dore and N. Aghanim, in preparation (2009).
- [23] A. Klypin, J. Holtzman, J. Primack, and E. Regos, *Astrophys. J.* **416**, 1 (1993), astro-ph/9305011.
- [24] J. R. Primack, J. Holtzman, A. Klypin, and D. O. Caldwell, *Phys. Rev. Lett.* **74**, 2160 (1995), astro-ph/9411020.
- [25] J. Brandbyge, S. Hannestad, T. Haugboelle, and B. Thomsen, *JCAP* **0808**, 020 (2008), 0802.3700.
- [26] J. Brandbyge and S. Hannestad (2008), 0812.3149.
- [27] F. Bernardeau, S. Colombi, E. Gaztanaga, and R. Scoccimarro, *Phys. Rept.* **367**, 1 (2002), astro-ph/0112551.
- [28] D. Jeong and E. Komatsu, *Astrophys. J.* **651**, 619 (2006), astro-ph/0604075.
- [29] D. Jeong and E. Komatsu (2008), 0805.2632.
- [30] M. Crocce and R. Scoccimarro, *Phys. Rev.* **D73**, 063519 (2006), astro-ph/0509418.
- [31] M. Crocce and R. Scoccimarro, *Phys. Rev.* **D77**, 023533 (2008), 0704.2783.
- [32] A. Taruya and T. Hiramatsu (2007), 0708.1367.
- [33] P. McDonald, *Phys. Rev.* **D75**, 043514 (2007), astro-ph/0606028.
- [34] S. Matarrese and M. Pietroni, *Mod. Phys. Lett.* **A23**, 25 (2008), astro-ph/0702653.
- [35] S. Matarrese and M. Pietroni, *JCAP* **0706**, 026 (2007), astro-ph/0703563.
- [36] K. Izumi and J. Soda, *Phys. Rev.* **D76**, 083517 (2007), 0706.1604.
- [37] T. Matsubara, *Phys. Rev.* **D77**, 063530 (2008), 0711.2521.
- [38] P. Valageas (2007), 0711.3407.
- [39] T. Matsubara, *Phys. Rev.* **D78**, 083519 (2008), 0807.1733.
- [40] M. Pietroni, *JCAP* **0810**, 036 (2008), 0806.0971.
- [41] S. Saito, M. Takada, and A. Taruya, *Phys. Rev. Lett.* **100**, 191301 (2008), 0801.0607.
- [42] Y. Y. Y. Wong, *JCAP* **0810**, 035 (2008), 0809.0693.
- [43] A. Lewis, A. Challinor, and A. Lasenby, *Astrophys. J.* **538**, 473 (2000), astro-ph/9911177.
- [44] H.-J. Seo, E. R. Siegel, D. J. Eisenstein, and M. White (2008), 0805.0117.